Original Article doi: 10.2176/nmc.oa.2021-0014

Neurol Med Chir (Tokyo) 61, 468–474, 2021 Online May 14, 2021

Streak Metal Artifact Reduction Technique in Cone Beam Computed Tomography Images after Endovascular Neurosurgery

Takafumi Otsuka,[1] Masahiro Nishihori,[1] Takashi Izumi,[1] Takeshi Uemura,[2] Takashi Sakai,[2] Mizuki Nakano,[1] Naoki Kato,[1] Fumiaki Kanamori,[1] Tetsuya Tsukada,[1] Kenji Uda,[1] Kinya Yokoyama,[1] Yoshio Araki,[1] and Ryuta Saito[1]

[1]*Department of Neurosurgery, Nagoya University Graduate School of Medicine, Nagoya, Aichi, Japan*

[2]*Radiological Technology, Department of Medical Technique, Nagoya University Hospital, Nagoya, Aichi, Japan*

Abstract

Cone beam computed tomography (CBCT) images are degraded by artifacts due to endovascular implants. We evaluated the use of streak metal artifact reduction technique (SMART) in non-contrast CBCT images after endovascular neurosurgery obtained from 148 patients (125 with aneurysm and 23 with dural arteriovenous fistula [dAVF]). Three neurosurgeons evaluated the cistern and brain surface visibility in CBCT images with and without SMART correction based on a 4-point scale (1, excellent; 2, good; 3, limited; and 4, insufficient). Significant improvement in visibility was achieved when the median scores improved from 4 or 3 to 2 or 1 or from 2 to 1. Metal artifact reduction in adjacent slices without metal and new artifacts after SMART correction was also examined. A significant improvement was achieved regarding the visibility of the cistern in 90 (60.8%) images and of the brain surface in 108 (73.0%) images. Metal size (cistern: odds ratio [OR], 0.91 per 1 mm increase; 95% confidence interval [CI], 0.83–0.99), irregular metal shape (cistern: OR, 0.18; 95% CI, 0.05–0.60 and brain surface: OR, 0.15; 95% CI, 0.05–0.45), and infratentorial lesions (cistern: OR, 0.37; 95% CI, 0.14–0.96 and brain surface: OR, 0.30; 95% CI, 0.11–0.80) were negatively correlated with improved visibility. Metal artifact reduction in adjacent slices without metal was obtained in 25.6% and 34.8% of images with aneurysm and dAVF, respectively. New artifacts after SMART correction were found in 4.8% and 13.0% of images with aneurysm and dAVF, respectively. SMART is especially effective for supratentorial small aneurysms.

Keywords: aneurysm, dural arteriovenous fistula, endovascular neurosurgery, non-contrast cone beam computed tomography, streak metal artifact reduction technique

Introduction

In recent years, the percentage of endovascular therapy for intracranial aneurysms has increased compared with that of open surgery due to the advancement in devices such as coils and stents. Endovascular therapy is less invasive than open surgery; the frequency of intraoperative rupture of intracranial aneurysms is reportedly lower in coil embolization than that in open surgery.[1)] However, once intraoperative rupture occurs during coil embolization, the risks of death and serious sequelae are higher.[1–3)] Therefore, complications such as periprocedural hemorrhage should be promptly detected and managed.[4,5)] At present, cone beam computed tomography (CBCT) is often used for the postoperative evaluation of endovascular therapy.[6)] CBCT can be performed in the angiography room without the need to move the patient. However, CBCT images are degraded by artifacts due to

Received January 18, 2021; Accepted March 23, 2021

cerebral endovascular and surgical implants such as coils, clips, and embolic substances, making it difficult to form an accurate diagnosis.

In 2010, Prell et al. reported a metal artifact reduction algorithm suitable for flat panel computed tomography (CT).[7] Thereafter, several studies have reported the use of metal artifact reduction algorithms for CBCT images after endovascular neurosurgery.[8–12] This study aimed to evaluate the efficacy of the streak metal artifact reduction technique (SMART), which is a modification and extension of previously reported metal artifact reduction algorithms and developed by Siemens Healthcare Sector, in non-contrast CBCT images after endovascular neurosurgery.

Methods

Patients

This retrospective analysis was approved by the Bioethics Review Committee of the Nagoya University Hospital. Informed consent for participation in this study was obtained from all patients. CBCT images obtained from 148 consecutive patients (mean age, 61.9 years; female, 89 [60.1%]; 125 with aneurysms and 23 with dural arteriovenous fistula [dAVF]) who underwent endovascular therapy between May 2017 and October 2019 were included. The patient characteristics are shown in Table 1. Cerebral aneurysms were treated with coil embolization with or without balloons and stents, and dAVFs were treated with coils or Onyx (Covidien, Irvine, CA, USA). Patients treated with flow diverter without coils were excluded.

Table 1 Baseline characteristics

	Value (%)
No. of patients	148
Mean age ± SD	61.9 ± 12.0
Female	89 (60.1)
Aneurysm	125
Mean size ± SD	8.2 ± 4.1
Location of aneurysm	
ICA	67 (53.6)
ACA	28 (22.4)
MCA	9 (7.2)
PCA	2 (1.6)
VBA	19 (15.2)
Treatment	
Simple dome embolization	78 (62.4)
Stent assist embolization	47 (37.6)
dAVF	23
Location of dAVF	
CS	10 (43.5)
TS	11 (47.8)
SSS	1 (4.3)
ACC	1 (4.3)
Treatment	
Coil embolization	17 (73.9)
ONYX	6 (26.1)

ACA: anterior cerebral artery, ACC: anterior condylar confluence, CS: cavernous sinus, ICA: internal carotid artery, MCA: middle cerebral artery, PCA: posterior cerebral artery, SSS: superior sagittal sinus, TS: transverse sinus, VBA: vertebra-basilar artery.

Image acquisition

CBCT images were taken using a biplane C-arm system (Siemens Artis QBA-Twin) based on a 20-s scan protocol with the following parameters: 109 kV, 200° rotation, without contrast medium. Image data were transferred to a clinical workstation *syngo* X-Workplace (VD20B; Siemens Healthcare GmbH, Forchheim Germany) and processed to reduce streak metal artifact using *syngo* DynaCT SMART (VD20B; Siemens Healthcare GmbH). Uncorrected and SMART-corrected CBCT axial images of 3-mm slice thickness were obtained. Both images had a pixel size of 512 × 512 and a voxel size of 027 × 0.27 × 0.27 mm.

Imaging evaluation

Three neurosurgeons (with 7, 7, and 8 years of experience) who were blinded to the patients' names and diseases were individually presented with uncorrected and SMART-corrected CBCT axial images including two slices containing metal core and two adjacent slices containing no metal. The visibility of the cistern and brain surfaces was evaluated using a 4-point scale (1: excellent, surrounding relevant anatomy is almost visible; 2: good visibility of the relevant anatomy, >50% of relevant anatomy is visible; 3: limited, <50% of relevant anatomy is visible; and 4: insufficient, almost invisible). An improvement in visibility was defined as an improvement in the median scores of three individuals from 4 or 3 to 2 or 1 or from 2 to 1. The effect of SMART in the two adjacent slices containing no metal and the appearance of new artifacts after SMART correction was also evaluated.

Statistical analysis

All data were expressed as mean and standard deviation. Intraclass correlations were used to assess inter-reader agreement. Score distribution between CBCT images with and without SMART correction

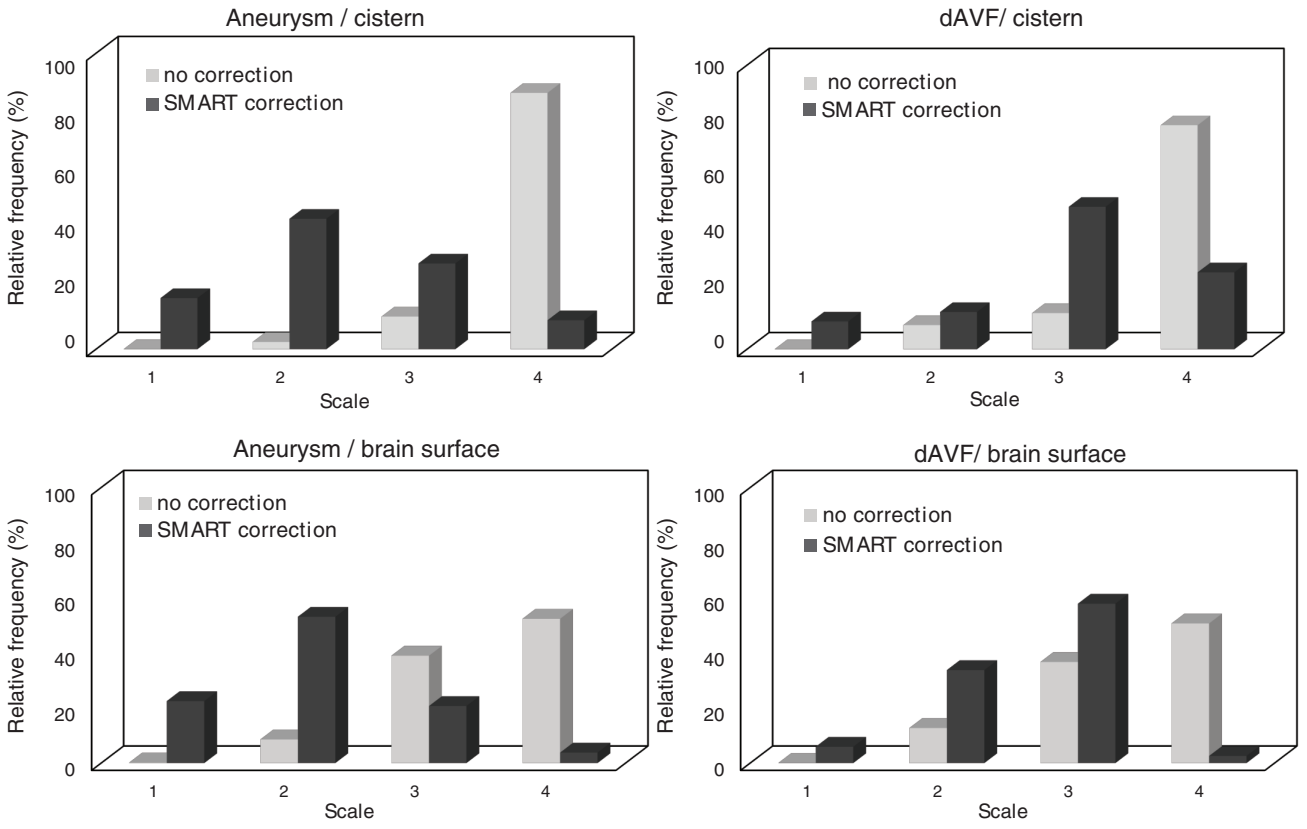

Fig. 1 Comparison of the distribution of the 4-point visibility scale in the cistern and brain surface of 125 patients with aneurysm and 23 with dAVF between uncorrected and SMART-corrected CBCT images. The distribution of 4-point scale in the cistern and brain surface of SMART-corrected CBCT images was found to be significantly different from that of uncorrected CBCT images in both patients with aneurysm and dAVF (P <0.001). CBCT: cone beam computed tomography, dAVF: dural arteriovenous fistula, SMART: streak metal artifact reduction technique.

was determined using the paired Wilcoxon signed-rank test. Factors related to significant improvement in visibility were analyzed using univariate and multivariate bionomical logistic regression analyses. Factors included in this analysis were age, sex, metal size, metal shape (spherical vs. irregular), and location (infratentorial vs. supratentorial). The metal size was defined as the maximal diameter in the axial slices. Transverse and sigmoid sinus dAVF were classified as infratentorial lesions. Factors with P values of <0.20 in univariate analysis were included in multivariate models. The threshold for significance was a P value of <0.05. All statistical analyses were performed using SPSS version 25 (IBM, Armonk, NY, USA).

Results

Visibility improvement

The inter-reader agreement in visibility scoring was almost perfect ($\alpha = 0.898$). Figure 1 shows the distribution of a 4-point visibility scale of CBCT images with and without SMART correction. In both cerebral aneurysms and dAVFs, the scale distribution of SMART-corrected images in the cistern and brain surface was found to be significantly different from that of uncorrected images (P <0.001). Regarding the visibility of the cistern, 90 (60.8%) of the 148 images showed a significant improvement: 86 (68.8%) of the 125 images with aneurysm and four (17.4%) of the 23 images with dAVF. Regarding the visibility of the brain surface, 108 (73.0%) of the 148 images showed a significant improvement: 102 (81.6%) of the 125 images with aneurysm and six (26.1%) of the 23 images with dAVF.

In the univariate analysis, metal size (cistern: OR, 0.87 per 1 mm increase; 95% CI, 0.80–0.94; P <0.001 and brain surface: OR, 0.87 per 1 mm increase; 95% CI, 0.80–0.93, P <0.001), irregular metal shape (cistern: OR, 0.10; 95% CI, 0.03–0.30; P <0.001 and brain surface: OR, 0.08; 95% CI, 0.03–0.22; P <0.001), and infratentorial lesions (cistern: OR, 0.24; 95% CI, 0.10–0.56; P <0.001 and brain surface: OR, 0.19; 95% CI, 0.08–0.44; P <0.001) were negatively associated with significantly improved visibility with SMART

Table 2 Results of univariate and multivariate binominal logistic regression analyses

(N, %)	Univariate		Multivariate	
	OR (95% CI)	P	OR (95% CI)	P
Age (year)	1.01 (0.98–1.04)/ 1.00 (0.97–1.03)	0.59/0.89	–	–
Female (89, 60.1)	0.78 (0.39–1.53)/ 1.16 (0.56–2.43)	0.47/0.69	–	–
Metal size (mm)	0.87 (0.80–0.94)/ 0.87 (0.80–0.93)	<0.001*/<0.001*	0.91 (0.83–0.99)/ 0.92 (0.84–1.01)	0.03*/0.06
Irregular shape (23, 15.5)	0.10 (0.03–0.30)/ 0.08 (0.03–0.22)	<0.001*/<0.001*	0.18 (0.05–0.60)/ 0.15 (0.05–0.45)	0.005*/0.001*
Infratentorial (30, 20.3)	0.24 (0.10–0.56)/ 0.19 (0.08–0.44)	0.001*/<0.001*	0.37 (0.14–0.96)/ 0.30 (0.11–0.80)	0.04*/0.02*

OR indicates odds ratio. P value and OR are expressed as values in cistern/brain surface. *P <0.05.

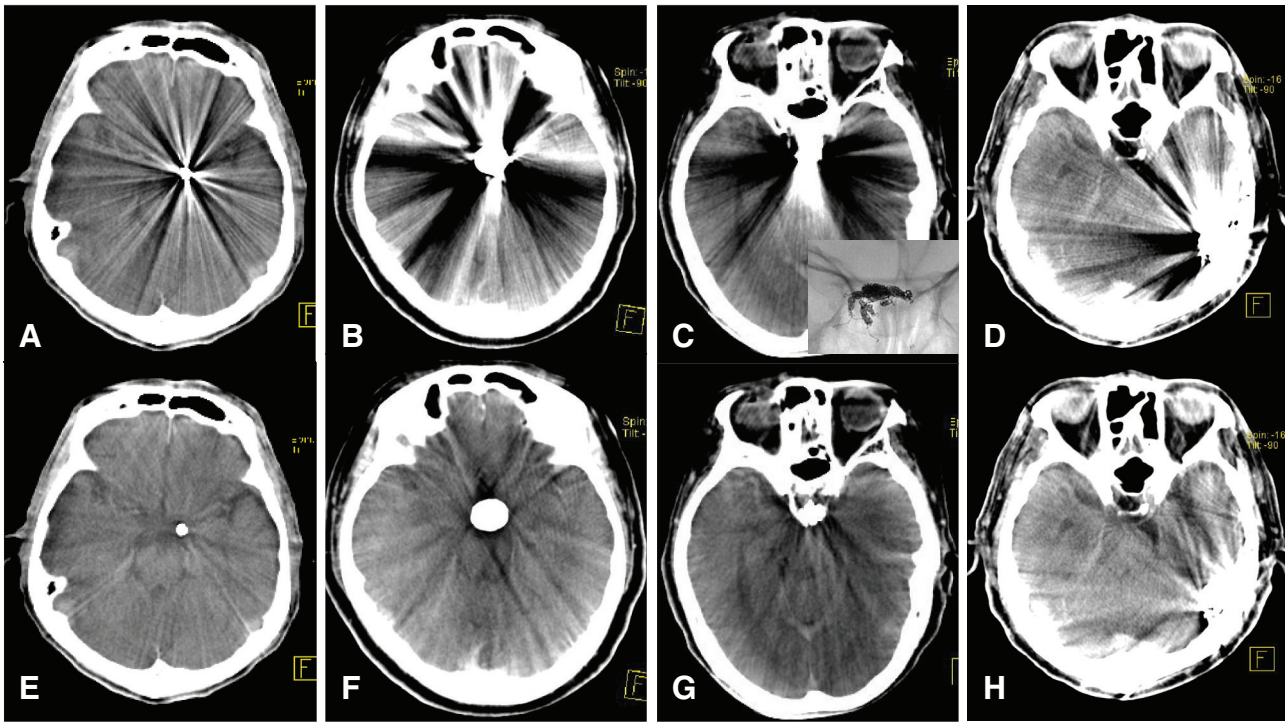

Fig. 2 Uncorrected (A–D) and its corresponding SMART-corrected (E–H) CBCT images. (A, E) Coil embolization of a 6-mm internal carotid artery aneurysm. The SMART-corrected image has drastically improved visibility compared with the uncorrected image. (B, F) Coil embolization of a 22-mm internal carotid artery aneurysm. Compared with small aneurysms, the effect of SMART was insufficient. (C, G) Coil embolization of the cavernous sinus dAVF. The superimposed image was intraoperative fluoroscopic image, which showed irregular shaped metal mass. The visibility improved, but not sufficient compared to small aneurysms. (D, H) Onyx embolization of the left transverse sinus dAVF. The visibility did not improve after SMART correction. CBCT: cone beam computed tomography, dAVF: dural arteriovenous fistula, SMART: streak metal artifact reduction technique.

correction. In the multivariate analysis, metal size (cistern: OR, 0.91 per 1 mm increase; 95% CI, 0.83–0.99; P = 0.026), irregular metal shape (cistern: OR, 0.18; 95% CI, 0.05–0.60; P = 0.005 and brain surface: OR, 0.15; 95% CI, 0.05–0.45; P = 0.001), and infratentorial lesions (cistern: OR, 0.37; 95% CI, 0.14–0.96; P = 0.042 and brain surface: OR, 0.30; 95% CI, 0.11–0.80; P = 0.016) were negatively associated with significantly improved visibility with SMART correction (Table 2, Fig. 2).

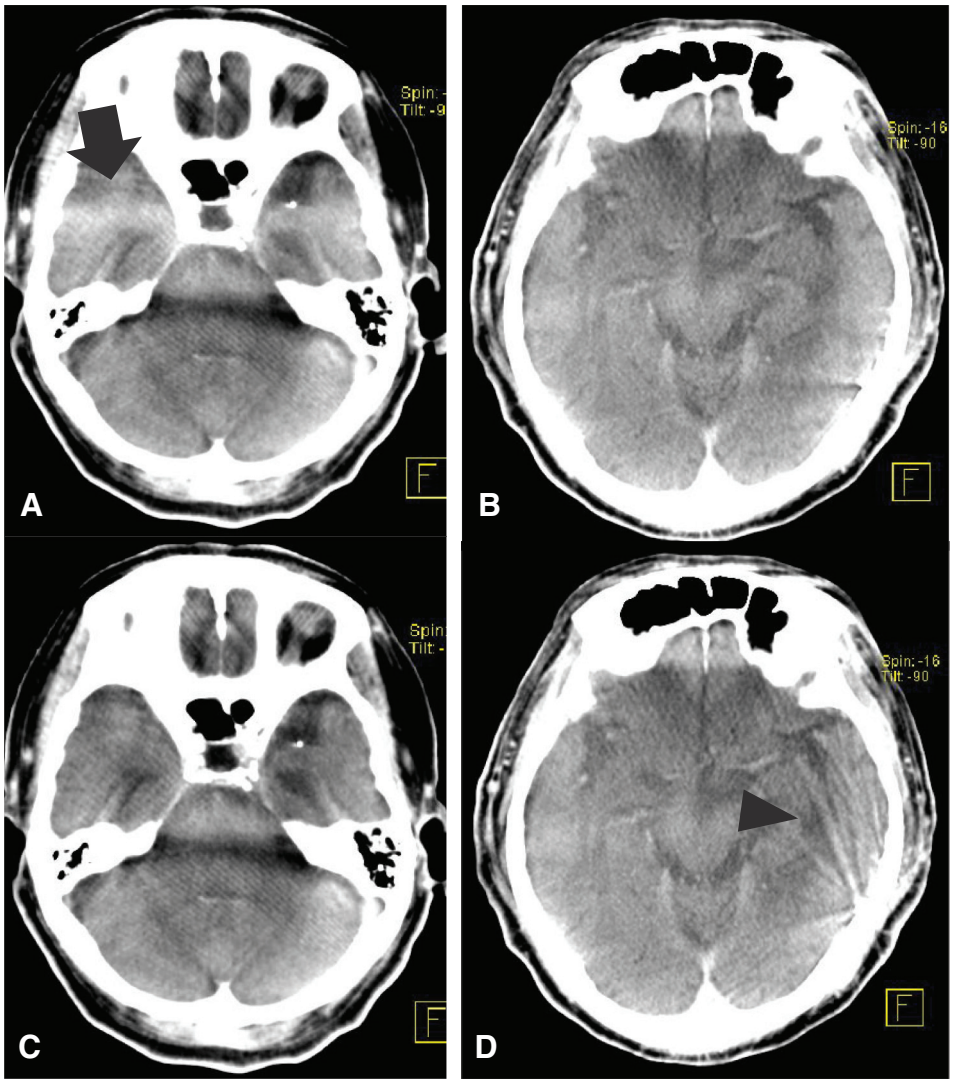

Fig. 3 Uncorrected (A, B) and its corresponding SMART-corrected (C, D) CBCT images. (A, C) Coil embolization of the left middle cerebral artery aneurysm. Metal artifact (arrow) was reduced in the adjacent plane without metal. (B, D) Coil embolization of left transverse sinus dAVF. New artifacts (arrow head) appeared after SMART correction. CBCT: cone beam computed tomography; dAVF: dural arteriovenous fistula; SMART: streak metal artifact reduction technique.

Metal artifact reduction in adjacent slices and new artifact after SMART correction

Regarding the metal artifact reduction in the adjacent slices without metal, the inter-reader agreement was substantial ($\alpha = 0.682$), and the reduction effect was observed in 32 (25.6%) of the 125 patients with aneurysm and eight (34.8%) of the 23 patients with dAVF. Regarding the appearance of new artifacts after SMART correction, the inter-reader agreement was moderate ($\alpha = 0.585$), and new artifacts appeared in 6 (4.8%) of the 125 patients with aneurysm and 3 (13.0%) of the 23 patients with dAVF. Figure 3 shows the illustrative cases of metal artifact reduction in adjacent slices (Fig. 3A and 3C) and new artifact after SMART correction (Fig. 3B and 3D).

Discussion

Dual-energy CT[13] and single-energy metal artifact reduction[14] are other metal artifact reduction techniques. However, these require transferring patients to a conventional CT scan, which delays the detection of complications and the time to intervention. Conversely, CBCT can be directly viewed with the AngioSuite. By applying metal artifact reduction on the CBCT image, the image quality can be improved, although the metal artifact cannot be completely removed. To date, several reports have used the metal artifact reduction prototype software, showing improved image quality to some extent in neuroendovascular cases.[8–12] The SMART algorithm consists of several

steps. First, the initial volume is reconstructed from the raw data containing metal artifacts. Then, the metal part is automatically segmented, creating a binary metal volume image. This binary metal volume is forward-projected onto the first reconstruction to identify data corrupted by artifacts. The corrupted data are interpolated by nonlinear procedure using the data along the metal region boundaries. A SMART-corrected image is reconstructed. Finally, the segmented metal part is overlaid.[11] This is the first report that used the commercial version of SMART software and included a number of patients higher than that in previous reports.[8–12] In addition, we focused on the shape and location of the implanted metal and evaluated whether these factors affect the visibility improvement by SMART. Therefore, we included dAVF cases, which often exhibit an irregular shaped metal mass after treatment.

SMART improved the visibility of non-contrast CBCT images after endovascular therapy in many cases with aneurysm. As shown in Fig. 2 A/E and B/F, SMART was more effective for smaller metal sizes. A previous study also reported that small aneurysms were associated with significantly improved visibility by metal artifact reduction technique.[8] In addition, spherical metal and supratentorial lesions were also associated with significantly improved image quality. Based on these results, SMART was the most effective for small and spherical supratentorial metal masses, that is, supratentorial small aneurysms, which are one of the most common pathologies in neurosurgery and are often treated with coil embolization. In addition, intraoperative rupture has been reported to more likely occur in small aneurysms than in large aneurysms.[15] Improving the visibility of the cistern around the aneurysm using SMART may improve the detectability of intraoperative rupture.

However, SMART did not significantly improve the visibility of the cistern and brain surface in the CBCT images of patients with dAVF. In multivariate analysis, SMART was not effective for viewing irregularly shaped metal masses. In addition, SMART was not effective in patients who underwent Onyx embolization (Fig. 2D and H). The first step performed by the SMART algorithm is identifying metal boundaries.[11] If the implanted metal is irregularly shaped, close to the bone, or with inhomogeneous structures like Onyx, the metal boundary definition process becomes difficult.[11] Furthermore, incorrect boundary definition has been reported to likely induce residual streak artifacts.[11] In the present study, new artifacts occurred more likely after SMART correction in the CBCT images of patients with dAVF. The metal boundary definition process performed by the SMART algorithm will need further improvement. At present, images before and after SMART correction should be compared and evaluated.

Metal artifacts in the adjacent slices without metal were reduced in 25.6% and 34.8% of images with aneurysm and dAVF, respectively. Based on our literature review, no report has addressed this. If metal artifact reduction can be achieved even in adjacent slices, complications might be more widely detected. Metal artifact reduction in the adjacent slices was slightly more common in CBCT images of dAVF because of the difficult metal boundary definition. The presented slice believed to contain no metal might still have contained a small amount of metal, which possibly induced overestimation of metal artifact reduction in the adjacent slices.

The inter-reader agreement was sufficient for the 4-point scale, but not good enough with respect to metal artifact reduction in the adjacent slices and appearance of new artifacts. As establishing clear criteria for these points is difficult, there was a lot of subjectivity in the evaluation, resulting in decreased inter-reader agreement.

There are several limitations to this study. First, this study was a single-center survey. Second, this study focused on assessing the visibility of CBCT images after SMART correction and did not investigate the detection of new findings masked by artifacts. All patients included in this study had unruptured aneurysms without intraoperative ruptures during the research period. Therefore, the ability to detect hemorrhages could not be evaluated. Third, 47 patients with aneurysms were treated with stent-assisted coiling; differences between coiling with and without stents were not examined. However, stents have been reported to barely cause artifacts; therefore, no benefit is expected from SMART correction.[12] Finally, we did not compare preoperative CT images with SMART-corrected CBCT images. Therefore, we could not evaluate the effect of SMART correction on the surrounding anatomy. However, our preliminary experiment using self-made phantom model demonstrates that SMART correction does not deform the surrounding anatomy.

Conclusion

SMART improved the visibility of CBCT images after endovascular therapy in many patients with cerebral aneurysm, but did not prove sufficient for CBCT images with dAVF. SMART was found to be particularly effective for small supratentorial aneurysms.

Acknowledgment

The software license of syngo DynaCT SMART was provided as a research material during the term of

collaboration research. The authors would like to thank Takahiro Imaizumi, affiliated to the Department of Advanced Medicine, Nagoya University Graduate School of Medicine, for assistance in statistical analysis.

Conflicts of Interest Disclosure

T.I. and M.N. received travel support from Siemens Healthcare, Co., Ltd to present the research result at a congress. The other authors have no conflicts of interest.

This study was partly funded by Siemens Healthcare, Co., Ltd under a collaboration research agreement with Department of Neurosurgery, Nagoya University.

References

1) Elijovich L, Higashida RT, Lawton MT, et al.: Predictors and outcomes of intraprocedural rupture in patients treated for ruptured intracranial aneurysms: the CARAT study. *Stroke* 39: 1501–1506, 2008
2) Cloft HJ, Kallmes DF: Cerebral aneurysm perforations complicating therapy with Guglielmi detachable coils: a meta-analysis. *AJNR Am J Neuroradiol* 23: 1706–1709, 2002
3) Imamura H, Sakai N, Sakai C, Fujinaka T, Ishii A: Endovascular treatment of aneurysmal subarachnoid hemorrhage in Japanese Registry of Neuroendovascular Therapy (JR-NET) 1 and 2. *Neurol Med Chir (Tokyo)* 54: 81–90, 2014
4) Stapleton CJ, Walcott BP, Butler WE, Ogilvy CS: Neurological outcomes following intraprocedural rerupture during coil embolization of ruptured intracranial aneurysms. *J Neurosurg* 122: 128–135, 2015
5) Tummala RP, Chu RM, Madison MT, Myers M, Tubman D, Nussbaum ES: Outcomes after aneurysm ruptured during endovascular coil embolization. *Neurosurgery* 49: 1059–1066, discussion 1066-1067, 2001
6) Psychogios MN, Buhk JH, Schramm P, et al.: Feasibility of angiographic CT in peri-interventional diagnostic imaging: a comparative study with multidetector CT. *AJNR Am J Neuroradiol* 31: 1226–1231, 2010
7) Prell D, Kalender WA, Kyriakou Y: Development, implementation and evaluation of a dedicated metal artefact reduction method for interventional flat-detector CT. *Br J Radiol* 83: 1052–1062, 2010
8) Enomoto Y, Yamauchi K, Asano T, Otani K, Iwama T: Effect of metal artifact reduction software on image quality of C-arm cone-beam computed tomography during intracranial aneurysm treatment. *Interv Neuroradiol* 24: 303–308, 2018
9) Prell D, Kyriakou Y, Struffert T, Dorfler A, Kalender WA: Metal artifact reduction for clipping and coiling in interventional C-arm CT. *AJNR Am J Neuroradiol* 31: 634–639, 2010
10) van der Bom IM, Hou SY, Puri AS, et al.: Reduction of coil mass artifacts in high-resolution flat detector conebeam CT of cerebral stent-assisted coiling. *AJNR Am J Neuroradiol* 34: 2163–2170, 2013
11) Stidd DA, Theessen H, Deng Y, et al.: Evaluation of a metal artifacts reduction algorithm applied to postinterventional flat panel detector CT imaging. *AJNR Am J Neuroradiol* 35: 2164–2169, 2014
12) Pjontek R, Önenköprülü B, Scholz B, et al.: Metal artifact reduction for flat panel detector intravenous CT angiography in patients with intracranial metallic implants after endovascular and surgical treatment. *J Neurointerv Surg* 8: 824–829, 2016
13) Mera Fernández D, Santos Armentia E, Bustos Fiore A, Villanueva Campos AM, Utrera Pérez E, Souto Bayarri M: The utility of dual-energy CT for metal artifact reduction from intracranial clipping and coiling. *Radiologia* 60: 312–319, 2018
14) Pan YN, Chen G, Li AJ, et al.: Reduction of metallic artifacts of the post-treatment intracranial aneurysms: effects of single energy metal artifact reduction algorithm. *Clin Neuroradiol* 29: 277–284, 2019
15) Kawabata S, Imamura H, Adachi H, et al.: Risk factors for and outcomes of intraprocedural rupture during endovascular treatment of unruptured intracranial aneurysms. *J Neurointerv Surg* 10: 362–366, 2018

Corresponding author: Masahiro Nishihori, MD
Department of Neurosurgery, Nagoya University Graduate School of Medicine, 65 Tsurumaicho, Showa-ku, Nagoya, Aichi, Japan.
e-mail: nishihori@med.nagoya-u.ac.jp